A Mouse Model for Metabolic Dysfunction-associated Steatotic Liver Disease and Hepatocellular Carcinoma

Byung-Kwan Jeong, Won-Il Choi, Wonsuk Choi, Jieun Moon, Won Hee Lee, Chan Choi, In Young Choi, Sang-Hyun Lee, Jung Kuk Kim, Young Seok Ju, Pilhan Kim, Young-Ah Moon, Jun Yong Park, Hail Kim

Table of contents

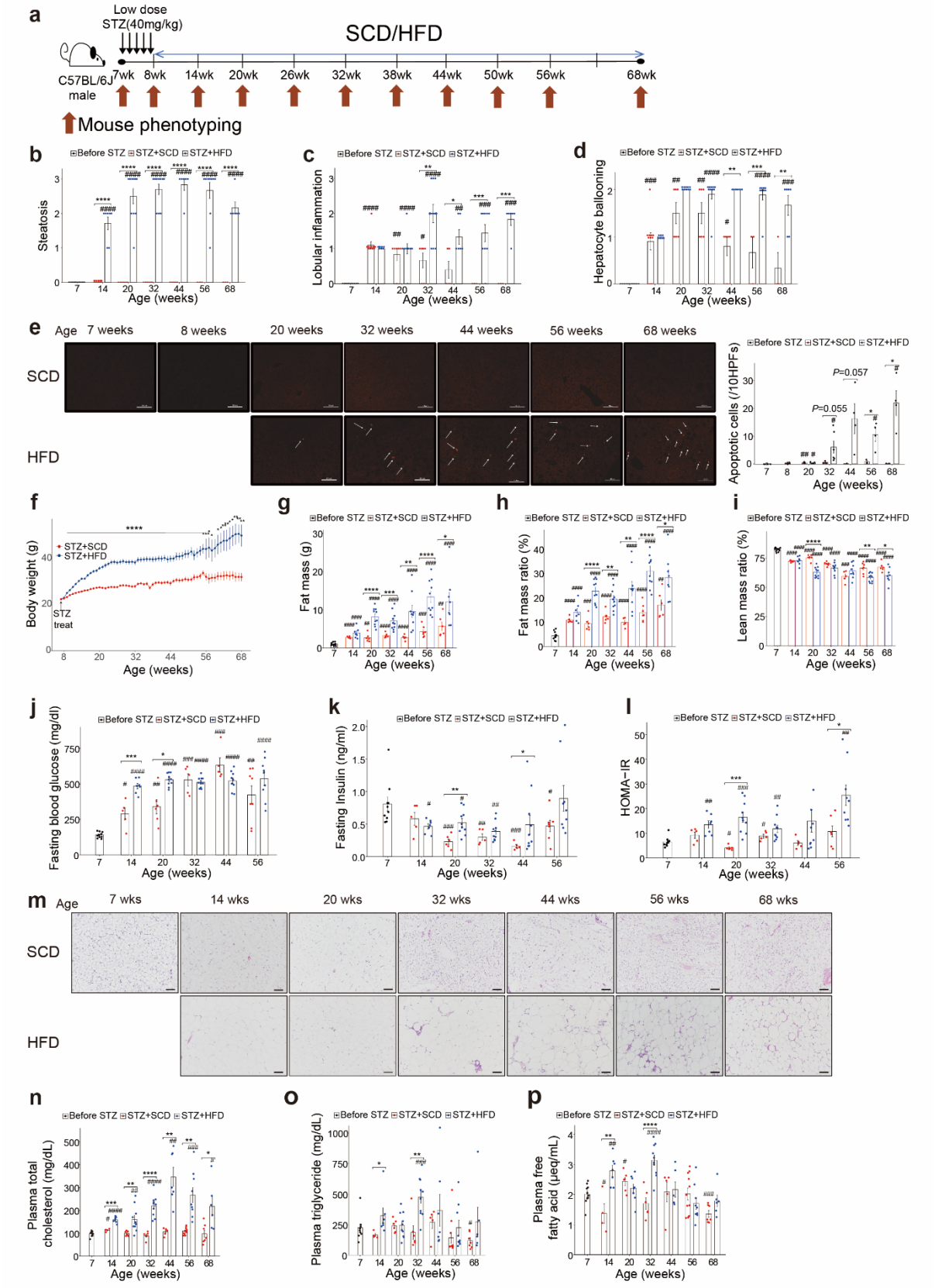
a
Low dose
STZ(40mg/kg)
SCD/HFD
C57BL/6J
male
7wk 8wk 14wk 20wk 26wk 32wk 38wk 44wk 50wk 56wk 68wk
Mouse phenotyping
b
Before STZ STZ+SCD STZ+HFD
Steatosis
Age (weeks)
c
Lobular inflammation
d
Hepatocyte ballooning
e
Age 7 weeks 8 weeks 20 weeks 32 weeks 44 weeks 56 weeks 68 weeks
SCD
HFD
Apoptotic cells (/10HPFs)
P=0.057
P=0.055
f
Body weight (g)
STZ+SCD
STZ+HFD
STZ treat
g
Fat mass (g)
h
Fat mass ratio (%)
i
Lean mass ratio (%)
j
Fasting blood glucose (mg/dl)
k
Fasting Insulin (ng/ml)
l
HOMA-IR
m
Age 7 wks 14 wks 20 wks 32 wks 44 wks 56 wks 68 wks
SCD
HFD
n
Plasma total cholesterol (mg/dL)
o
Plasma triglyceride (mg/dL)
p
Plasma free fatty acid (μeq/mL)

Supplementary Fig. 1. Hepatic and metabolic phenotypes of STZ+HFD mice. (a-p) Seven-week-old B6J mice were treated with STZ and fed SCD or HFD for 6-60 weeks. **(a)** Schematic illustration. **(b-d)** Detailed NAFLD activity scores (NAS) using the NASH CRN scoring system; Before STZ treatment, *n*= 10; STZ+SCD, *n*= 10, 6, 6, 5, 3, and 3, from 14 to 68-week-old, respectively; STZ+HFD, *n*= 7, 10, 10, 6, 9, and 6, from 14 to 68-week-old, respectively. **(e)** Immunofluorescent terminal deoxynucleotidyl transferase dUTP nick end labeling (TUNEL) of STZ-treated mouse liver, with apoptotic cell counts. Arrows signify apoptotic cells. Scale bar, 100 μm; Before STZ treatment, *n*= 5; STZ+SCD, *n*= 5, 4, 3, 3, 3, and 3, from 8 to 68-week-old, respectively; STZ+HFD, *n*= 5, 6, 4, 4, and 4, from 20 to 68-week-old, respectively. **(f)** Body weight trends; $n \geq 6$ per group. **(g-i) (g)** Fat mass weight, **(h)** percentage fat body mass and **(i)** lean body mass of STZ-treated mice; Before STZ treatment, *n*= 10; STZ+SCD, *n*= 5, 6, 6, 5, 7, and 6, from 14 to 68-week-old, respectively; STZ+HFD, *n*= 7, 10, 10, 9, 10, and 8, from 14 to 68-week-old, respectively. **(j-l) (j)** Fasting blood glucose, **(k)** Fasting plasma insulin and **(l)** HOMA-IR levels of STZ-treated mice; Before STZ treatment, *n*= 10; STZ+SCD, *n*= 5, 6, 6, 5, and 7, from 14 to 56-week-old, respectively; STZ+HFD, *n*= 7, 10, 10, 10, and 9, from 14 to 56-week-old, respectively. **(m)** Representative eWAT via H&E staining. Scale bar, 100 μm. **(n-p)** Plasma **(n)** total cholesterol, **(o)** triglyceride and **(p)** free fatty acid levels; Before STZ treatment, *n*= 10; STZ+SCD, *n*= 4, 6, 6, 5, 11, and 7, from 14 to 68-week-old, respectively; STZ+HFD, *n*= 7, 10, 10, 7, 9, and 6, from 14 to 68-week-old, respectively. Data are expressed as means ± SEM. $^{*}P<0.05$, $^{**}P<0.01$, $^{***}P<0.001$, $^{****}P<0.0001$, compared with age-matched group, Student's t-test or Welch's t-test **(b-l, n-p)**. $^{\#}P<0.05$, $^{\#\#}P<0.01$, $^{\#\#\#}P<0.001$, $^{\#\#\#\#}P<0.0001$, compared with 7-week-old control group, Student's t-test or Welch's t-test **(b-l, n-p)**. Source data are provided as a Source Data file.

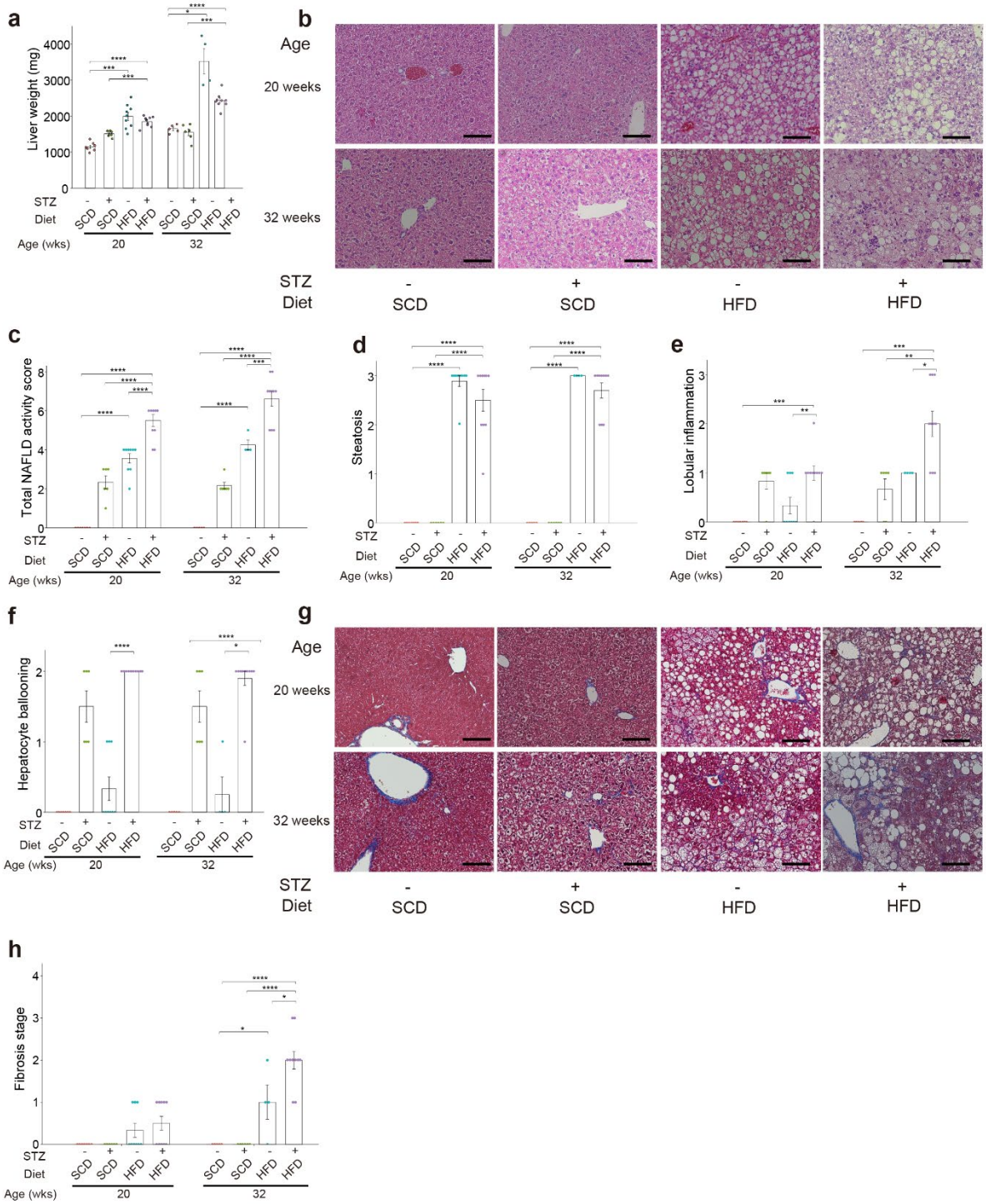
a
Liver weight (mg)
4000
3000
2000
1000
0
STZ
Diet
Age (wks)
SCD
HFD
20
32
b
Age
20 weeks
32 weeks
STZ
Diet
SCD
HFD
c
Total NAFLD activity score
d
Steatosis
e
Lobular inflammation
f
Hepatocyte ballooning
g
h
Fibrosis stage

Supplementary Fig. 2. Hepatic phenotype assessment in four mouse groups at 20 and 32 weeks of age. (a-h) Seven-week-old B6J mice were treated with STZ or not, and fed SCD or HFD for 12-24 weeks from eight weeks of age. **(a)** Liver weight; *n*= 7, 6, 9, 9, 5, 6, 4, and 9 from left to right in the bar graph. **(b)** Representative liver histology evaluated via H&E staining. Scale bar, 100 μm. The data are representative results of the biological replicates shown in **(c-f) (c-f)** Nonalcoholic fatty liver disease score (NAS) and detailed NAS graded using the NASH CRN scoring system; *n*= 7, 6, 9, 10, 5, 6, 4, and 10 from left to right in each bar graph, respectively. **(g)** Representative liver histology evaluated via Masson's trichrome staining for hepatic fibrosis. Scale bar, 100 μm. The data are representative results of the biological replicates shown in **(h).** (**h**) Fibrosis stage graded using the NASH CRN scoring system; *n*= 7, 6, 9, 10, 5, 6, 4, and 10 from left to right in the bar graph. Data are expressed as means ± SEM. $^{*}P<0.05$, $^{**}P<0.01$, $^{***}P<0.001$, $^{****}P<0.0001$, one-way ANOVA with post-hoc Tukey's test or Welch's ANOVA with post-hoc Games-Howell test among age-matched groups **(a, c-f, h).** Source data are provided as a Source Data file.

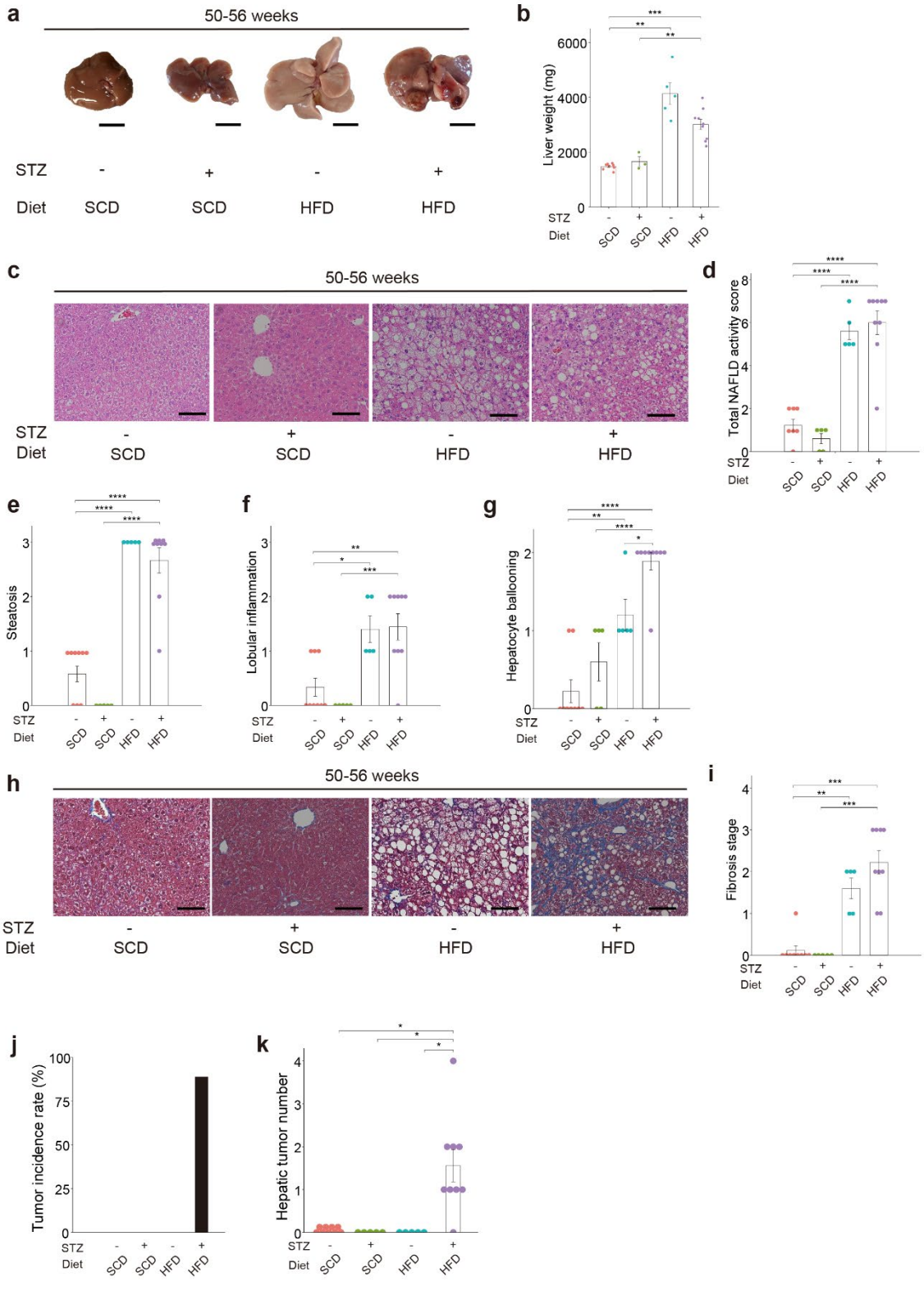
a
50-56 weeks
STZ - + - +
Diet SCD SCD HFD HFD
b
Liver weight (mg)
c
50-56 weeks
d
Total NAFLD activity score
e
Steatosis
f
Lobular inflammation
g
Hepatocyte ballooning
h
50-56 weeks
i
Fibrosis stage
j
Tumor incidence rate (%)
k
Hepatic tumor number

Supplementary Fig. 3. Hepatic phenotype assessment in four mouse groups at 50-56 weeks of age. (a-k) Seven-week-old B6J mice were treated with STZ or not, and fed SCD or HFD for 42-48 weeks from eight weeks of age. **(a)** Representative liver gross image of different groups of mice at 50-56 weeks of age. Scale bar, 1 cm. The data are representative results of 5 biological replicates of each group. **(b)** Liver weight; *n*= 9, 3, 5, and 9 from left to right in the bar graph. **(c)** Representative liver histology evaluated via H&E staining. Scale bar, 100 μm. The data are representative results of the biological replicates shown in **(d-g)**. **(d-g)** Nonalcoholic fatty liver disease score (NAS) graded using the NASH CRN scoring system; *n*= 9, 5, 5, and 9 from left to right in each bar graph, respectively. **(h)** Representative liver histology evaluated by Masson's trichrome staining for hepatic fibrosis. Scale bar, 100 μm. The data are representative results of the biological replicates shown in **(i). (i)** Fibrosis stage graded using the NASH CRN scoring system; *n*= 9, 5, 5, and 9 from left to right in the bar graph. **(j, k)** Hepatic tumor **(j)** incidence and **(k)** number; *n*= 9, 5, 5, and 9 from left to right in the bar graph. Data are expressed as means ± SEM. $^{*}P<0.05$, $^{**}P<0.01$, $^{***}P<0.001$, $^{****}P<0.0001$, one-way ANOVA with post-hoc Tukey's test or Welch's ANOVA with post-hoc Games-Howell test according to homogeneity of variance among age-matched groups (**d-g, i, k**). Source data are provided as a Source Data file.

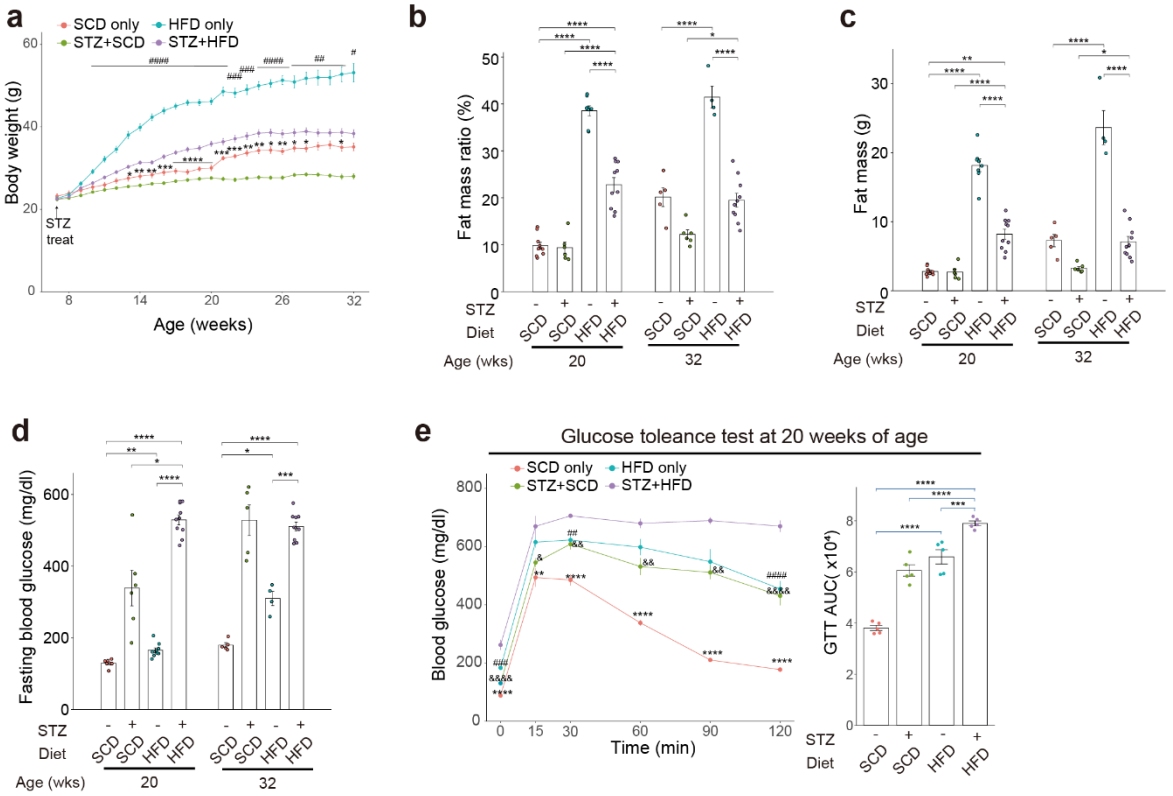

Supplementary Fig. 4. Metabolic phenotype assessment in four mouse groups at 20 and 32 weeks of age. (a-e) Seven-week-old B6J mice were treated with STZ or not, and fed SCD or HFD for 12-24 weeks from eight weeks of age. **(a)** Body weight trends**;** $n \geq 4$ per group (*: STZ+HFD compared to SCD-only; $^{\#}$: STZ+HFD compared to HFD-only). **(b, c) (b)** Percentage fat body mass and **(c)** fat mass weight; n= 10, 6, 8, 10, 5, 6, 4, and 10 from left to right in each bar graph, respectively. **(d)** Blood glucose levels after 6 h of fasting; n= 10, 6, 10, 10, 5, 5, 4, and 10 from left to right in the bar graph. **(e)** Intraperitoneal glucose tolerance test (IPGTT) after 14 h of fasting at 20 weeks of age (*: STZ+HFD compared to SCD-only; $^{\#}$: STZ+HFD compared to HFD-only; $^{\&}$: STZ+HFD compared to STZ+SCD); n = 5 per group. Data are expressed as means ± SEM. $^{*,\#,\&}P<0.05$, $^{**,\#\#,\&\&}P<0.01$, $^{***,\#\#\#,\&\&\&}P<0.001$, $^{****,\#\#\#\#,\&\&\&\&}P<0.0001$, one-way ANOVA with post-hoc Tukey's test or Welch's ANOVA with post-hoc Games-Howell test according to homogeneity of variance among age-matched groups (**a-e**). Source data are provided as a Source Data file.

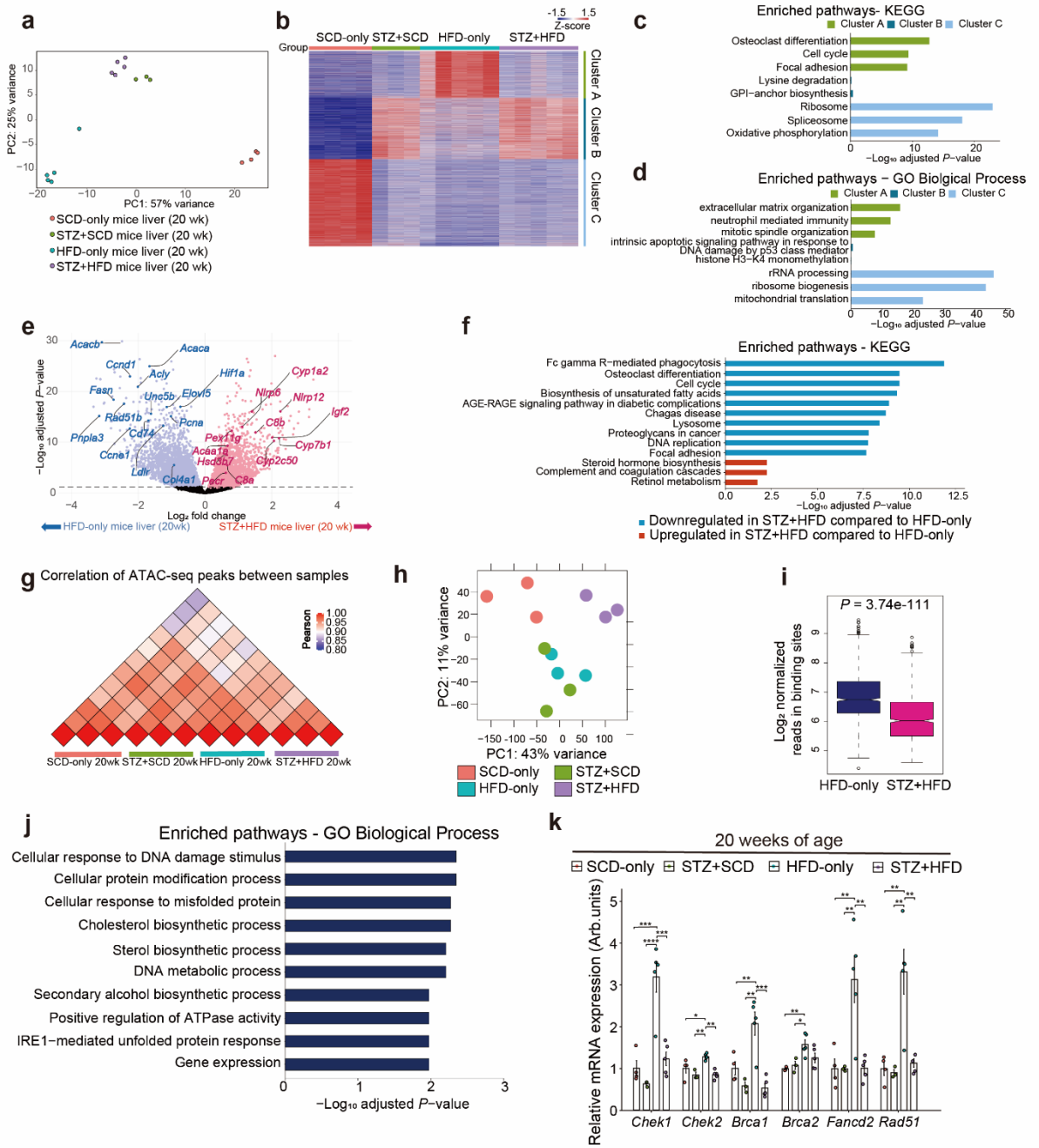
a
PC2: 25% variance
PC1: 57% variance
SCD-only mice liver (20 wk)
STZ+SCD mice liver (20 wk)
HFD-only mice liver (20 wk)
STZ+HFD mice liver (20 wk)
b
Z-score
Group
SCD-only STZ+SCD HFD-only STZ+HFD
Cluster A Cluster B Cluster C
c
Enriched pathways- KEGG
Cluster A Cluster B Cluster C
Osteoclast differentiation
Cell cycle
Focal adhesion
Lysine degradation
GPI−anchor biosynthesis
Ribosome
Spliceosome
Oxidative phosphorylation
−Log10 adjusted P−value
d
Enriched pathways − GO Biolgical Process
Cluster A Cluster B Cluster C
extracellular matrix organization
neutrophil mediated immunity
mitotic spindle organization
intrinsic apoptotic signaling pathway in response to DNA damage by p53 class mediator
histone H3−K4 monomethylation
rRNA processing
ribosome biogenesis
mitochondrial translation
−Log10 adjusted P−value
e
−Log10 adjusted P−value
Log2 fold change
HFD-only mice liver (20wk)
STZ+HFD mice liver (20 wk)
Acacb
Acaca
Ccnd1
Acly
Hif1a
Cyp1a2
Fasn
Unc5b
Elovl5
Nlrp6
Nlrp12
Igf2
Rad51b
Pcna
C8b
Pnpla3
Cd14
Pex11g
Cyp7b1
Ccne1
Acaa1a
Hsd3b7
Cyp2c50
Ldlr
Col4a1
Pecr
C8a
f
Enriched pathways - KEGG
Fc gamma R−mediated phagocytosis
Osteoclast differentiation
Cell cycle
Biosynthesis of unsaturated fatty acids
AGE-RAGE signaling pathway in diabetic complications
Chagas disease
Lysosome
Proteoglycans in cancer
DNA replication
Focal adhesion
Steroid hormone biosynthesis
Complement and coagulation cascades
Retinol metabolism
−Log10 adjusted P−value
Downregulated in STZ+HFD compared to HFD-only
Upregulated in STZ+HFD compared to HFD-only
g
Correlation of ATAC-seq peaks between samples
Pearson
SCD-only 20wk STZ+SCD 20wk HFD-only 20wk STZ+HFD 20wk
h
PC2: 11% variance
PC1: 43% variance
SCD-only
STZ+SCD
HFD-only
STZ+HFD
i
P = 3.74e-111
Log2 normalized reads in binding sites
HFD-only STZ+HFD
j
Enriched pathways - GO Biological Process
Cellular response to DNA damage stimulus
Cellular protein modification process
Cellular response to misfolded protein
Cholesterol biosynthetic process
Sterol biosynthetic process
DNA metabolic process
Secondary alcohol biosynthetic process
Positive regulation of ATPase activity
IRE1−mediated unfolded protein response
Gene expression
−Log10 adjusted P−value
k
20 weeks of age
SCD-only STZ+SCD HFD-only STZ+HFD
Relative mRNA expression (Arb.units)
Chek1 Chek2 Brca1 Brca2 Fancd2 Rad51

Supplementary Fig. 5. STZ+HFD mouse liver loss of compensatory responses to liver damage. (a-k) Liver RNA and ATAC-seq profiling was performed in 20-week-old B6J mice, categorized by HFD intake and STZ treatment. **(a)** Principal component analyses of liver RNA-seq data. **(b)** K-means clustering of differentially expressed genes among 20-week-old mice. **(c, d)** Functional enrichment analyses using **(c)** KEGG and **(d)** GO biological process pathways for each gene cluster. **(e)** Volcano plot comparing STZ+HFD mouse liver samples to HFD-only mouse liver samples. **(f)** Functional enrichment analyses based on KEGG pathways of STZ+HFD mouse liver samples compared with HFD-only mouse liver samples. **(g)** Similarity heatmap demonstrating Pearson correlation of normalized ATAC-seq reads (consensus peak sites) from liver. **(h)** Principal component analyses of ATAC-seq data. **(i)** Normalized ATAC-seq reads of all sites from STZ+HFD and HFD-only mice. The box limits indicate the upper and lower quartiles, covering the interquartile range, whiskers extend to 1.5 times the interquartile range, and individual points beyond the whiskers denote outliers. **(j)** Functional enrichment analyses using GO biological process pathways for repressed chromatin binding site-overlapping genes in STZ+HFD compared to HFD-only mice. **(k)** Relative expression (normalized reads from RNA-seq data) of genes related to DNA double-strand break repair via homologous recombination in livers from 20-week-old mice; n = 5 for SCD-only, 3 for STZ+SCD, 5 for HFD-only, and 5 for STZ+HFD (Arb. units; arbitrary units). Data are expressed as means ± SEM. $^{*}P<0.05$, $^{**}P<0.01$, $^{***}P<0.001$, compared with age-matched group, one-way ANOVA with post hoc Tukey's test **(k)**. Source data are provided as a Source Data file.

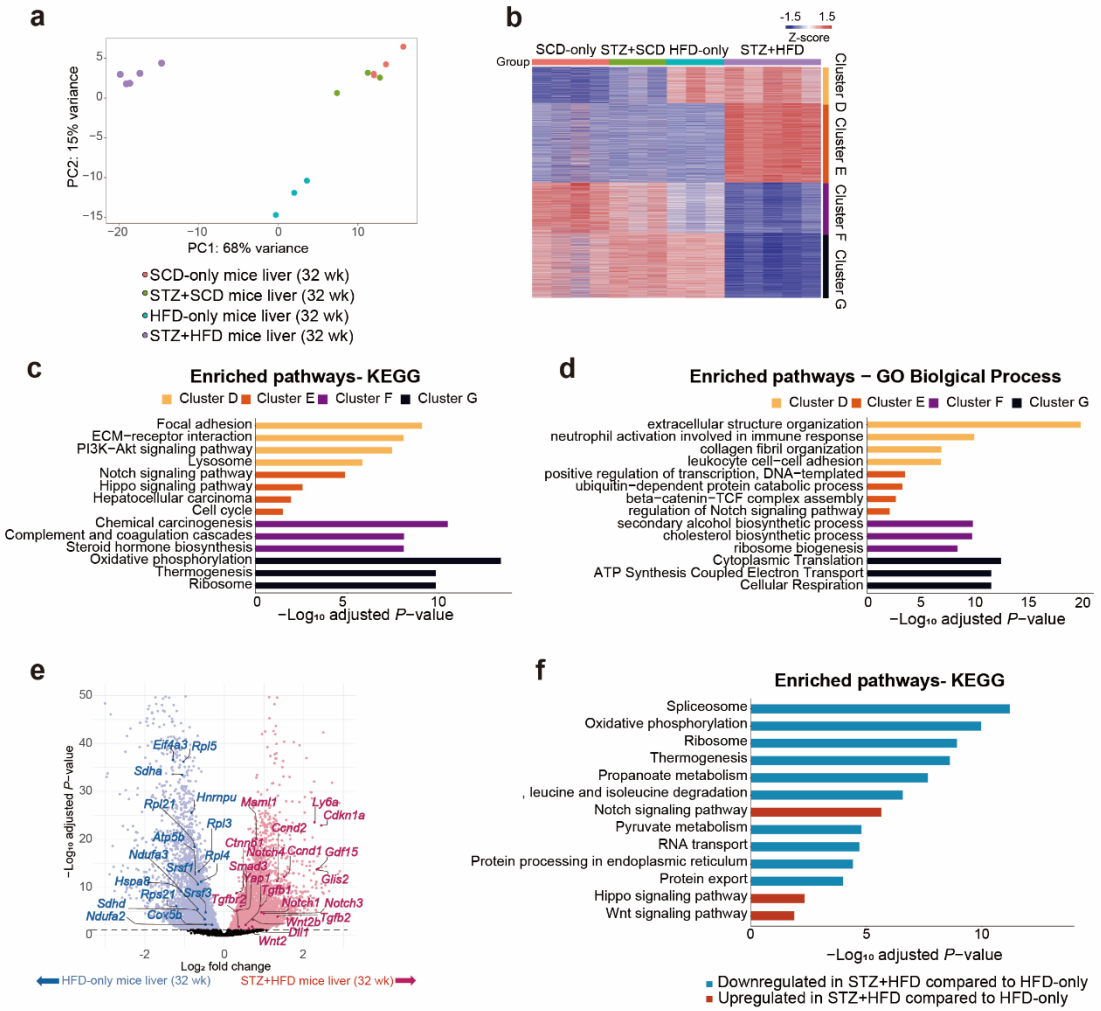
a
PC2: 15% variance
PC1: 68% variance
SCD-only mice liver (32 wk)
STZ+SCD mice liver (32 wk)
HFD-only mice liver (32 wk)
STZ+HFD mice liver (32 wk)
b
Z-score
Group
SCD-only STZ+SCD HFD-only STZ+HFD
Cluster D Cluster E Cluster F Cluster G
c
Enriched pathways- KEGG
Cluster D Cluster E Cluster F Cluster G
Focal adhesion
ECM−receptor interaction
PI3K−Akt signaling pathway
Lysosome
Notch signaling pathway
Hippo signaling pathway
Hepatocellular carcinoma
Cell cycle
Chemical carcinogenesis
Complement and coagulation cascades
Steroid hormone biosynthesis
Oxidative phosphorylation
Thermogenesis
Ribosome
−Log₁₀ adjusted P−value
d
Enriched pathways − GO Biolgical Process
Cluster D Cluster E Cluster F Cluster G
extracellular structure organization
neutrophil activation involved in immune response
collagen fibril organization
leukocyte cell−cell adhesion
positive regulation of transcription, DNA−templated
ubiquitin−dependent protein catabolic process
beta−catenin−TCF complex assembly
regulation of Notch signaling pathway
secondary alcohol biosynthetic process
cholesterol biosynthetic process
ribosome biogenesis
Cytoplasmic Translation
ATP Synthesis Coupled Electron Transport
Cellular Respiration
−Log₁₀ adjusted P−value
e
−Log₁₀ adjusted P−value
Log₂ fold change
HFD-only mice liver (32 wk)
STZ+HFD mice liver (32 wk)
f
Enriched pathways- KEGG
Spliceosome
Oxidative phosphorylation
Ribosome
Thermogenesis
Propanoate metabolism
, leucine and isoleucine degradation
Notch signaling pathway
Pyruvate metabolism
RNA transport
Protein processing in endoplasmic reticulum
Protein export
Hippo signaling pathway
Wnt signaling pathway
−Log₁₀ adjusted P−value
Downregulated in STZ+HFD compared to HFD-only
Upregulated in STZ+HFD compared to HFD-only

Supplementary Fig. 6. Hepatic transcriptomic analysis in four mouse groups at 32 weeks of age. (a-f) Liver RNA-seq profiling was performed in 32-week-old B6J mice, categorized by HFD intake and STZ treatment. **(a)** Principal component analyses of liver RNA-seq data. **(b)** K-means clustering of differentially expressed genes among 32-week-old mice. **(c, d)** Functional enrichment analyses using **(c)** KEGG and **(d)** GO biological process pathways for each gene cluster. **(e)** Volcano plot comparing STZ+HFD mouse liver samples to HFD-only mouse liver samples. **(f)** Functional enrichment analyses based on KEGG pathways of STZ+HFD mouse liver samples compared with HFD-only mouse liver samples.

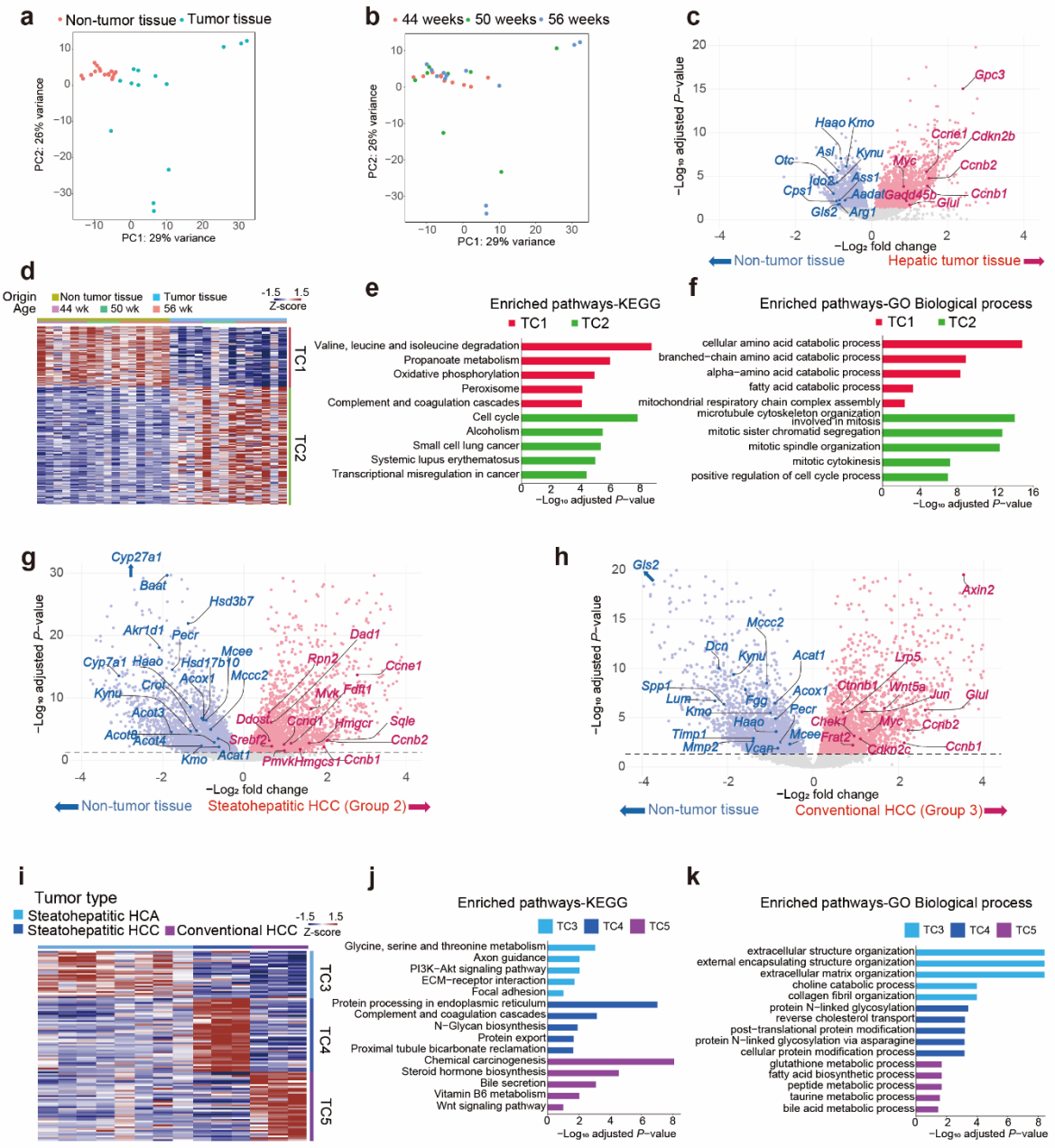
a
Non-tumor tissue
Tumor tissue
PC2: 26% variance
PC1: 29% variance
b
44 weeks
50 weeks
56 weeks
PC2: 26% variance
PC1: 29% variance
c
−Log₁₀ adjusted P−value
−Log₂ fold change
Non-tumor tissue
Hepatic tumor tissue
Gpc3
Haao
Kmo
Ccne1
Cdkn2b
Asl
Kynu
Otc
Myc
Ccnb2
Ido2
Ass1
Cps1
Aadat
Gadd45b
Ccnb1
Gls2
Arg1
Glul
d
Origin
Age
Non tumor tissue
Tumor tissue
44 wk
50 wk
56 wk
Z-score
TC1
TC2
e
Enriched pathways-KEGG
TC1
TC2
Valine, leucine and isoleucine degradation
Propanoate metabolism
Oxidative phosphorylation
Peroxisome
Complement and coagulation cascades
Cell cycle
Alcoholism
Small cell lung cancer
Systemic lupus erythematosus
Transcriptional misregulation in cancer
−Log₁₀ adjusted P−value
f
Enriched pathways-GO Biological process
TC1
TC2
cellular amino acid catabolic process
branched−chain amino acid catabolic process
alpha−amino acid catabolic process
fatty acid catabolic process
mitochondrial respiratory chain complex assembly
microtubule cytoskeleton organization involved in mitosis
mitotic sister chromatid segregation
mitotic spindle organization
mitotic cytokinesis
positive regulation of cell cycle process
−Log₁₀ adjusted P−value
g
−Log₁₀ adjusted P−value
−Log₂ fold change
Non-tumor tissue
Steatohepatitic HCC (Group 2)
Cyp27a1
Baat
Hsd3b7
Akr1d1
Pecr
Mcee
Cyp7a1
Haao
Hsd17b10
Acox1
Mccc2
Rpn2
Dad1
Ccne1
Kynu
Crot
Mvk
Fdft1
Acot3
Ddost
Ccnd1
Hmgcr
Sqle
Acot8
Acot4
Srebf2
Ccnb2
Kmo
Acat1
Pmvk
Hmgcs1
Ccnb1
h
−Log₁₀ adjusted P−value
−Log₂ fold change
Non-tumor tissue
Conventional HCC (Group 3)
Gls2
Axin2
Mccc2
Dcn
Kynu
Acat1
Lrp5
Spp1
Lum
Fgg
Acox1
Ctnnb1
Wnt5a
Jun
Glul
Kmo
Haao
Pecr
Chek1
Myc
Ccnb2
Timp1
Mmp2
Vcan
Mcee
Frat2
Cdkn2c
Ccnb1
i
Tumor type
Steatohepatitic HCA
Steatohepatitic HCC
Conventional HCC
Z-score
TC3
TC4
TC5
j
Enriched pathways-KEGG
TC3
TC4
TC5
Glycine, serine and threonine metabolism
Axon guidance
PI3K−Akt signaling pathway
ECM−receptor interaction
Focal adhesion
Protein processing in endoplasmic reticulum
Complement and coagulation cascades
N−Glycan biosynthesis
Protein export
Proximal tubule bicarbonate reclamation
Chemical carcinogenesis
Steroid hormone biosynthesis
Bile secretion
Vitamin B6 metabolism
Wnt signaling pathway
−Log₁₀ adjusted P−value
k
Enriched pathways-GO Biological process
TC3
TC4
TC5
extracellular structure organization
external encapsulating structure organization
extracellular matrix organization
choline catabolic process
collagen fibril organization
protein N−linked glycosylation
reverse cholesterol transport
post−translational protein modification
protein N−linked glycosylation via asparagine
cellular protein modification process
glutathione metabolic process
fatty acid biosynthetic process
peptide metabolic process
taurine metabolic process
bile acid metabolic process
−Log₁₀ adjusted P−value

Supplementary Fig. 7. Transcriptomic characteristics of hepatic tumors in STZ+HFD mice according to tumor type. (a-k) RNA-seq profiling was performed on hepatic tumor and non-tumor liver tissues of 44 to 56-week-old STZ+HFD mice. **(a, b)** Principal component analyses of RNA-seq data grouped by **(a)** tumor presence and **(b)** age. **(c)** Volcano plot comparing tumor and non-tumor tissue samples. **(d)** K-means clustering of differentially expressed genes between tumor and non-tumor tissue samples. **(e, f)** Functional enrichment analyses using **(e)** KEGG and **(f)** GO biological process pathways for each gene cluster. **(g, h)** Volcano plot comparing tumors resembling **(g)** steatohepatitic HCC (Group 2) or **(h)** conventional HCC (Group 3) to non-tumor tissue. **(i)** K-means clustering of differentially expressed genes among tumor groups in STZ+HFD mice. **(j, k)** Functional enrichment analyses using **(j)** KEGG and **(k)** GO biological process pathways for each gene cluster.

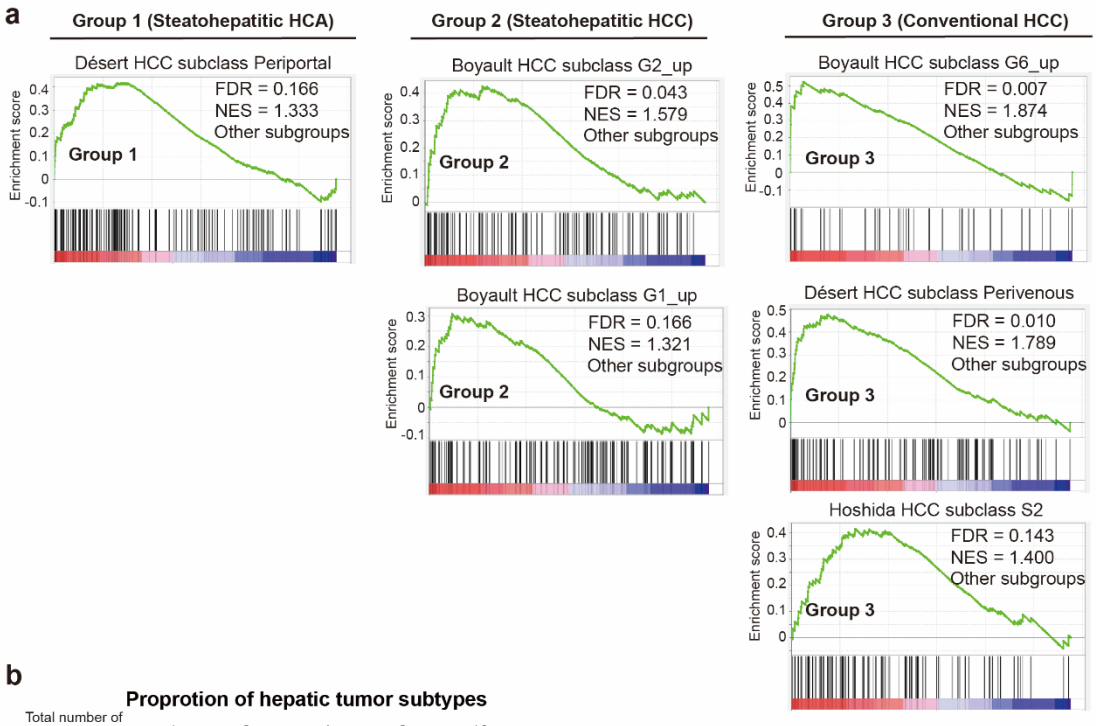
a
Group 1 (Steatohepatitic HCA)
Group 2 (Steatohepatitic HCC)
Group 3 (Conventional HCC)
Désert HCC subclass Periportal
FDR = 0.166
NES = 1.333
Other subgroups
Group 1
Boyault HCC subclass G2_up
FDR = 0.043
NES = 1.579
Other subgroups
Group 2
Boyault HCC subclass G6_up
FDR = 0.007
NES = 1.874
Other subgroups
Group 3
Boyault HCC subclass G1_up
FDR = 0.166
NES = 1.321
Other subgroups
Group 2
Désert HCC subclass Perivenous
FDR = 0.010
NES = 1.789
Other subgroups
Group 3
Hoshida HCC subclass S2
FDR = 0.143
NES = 1.400
Other subgroups
Group 3
Enrichment score

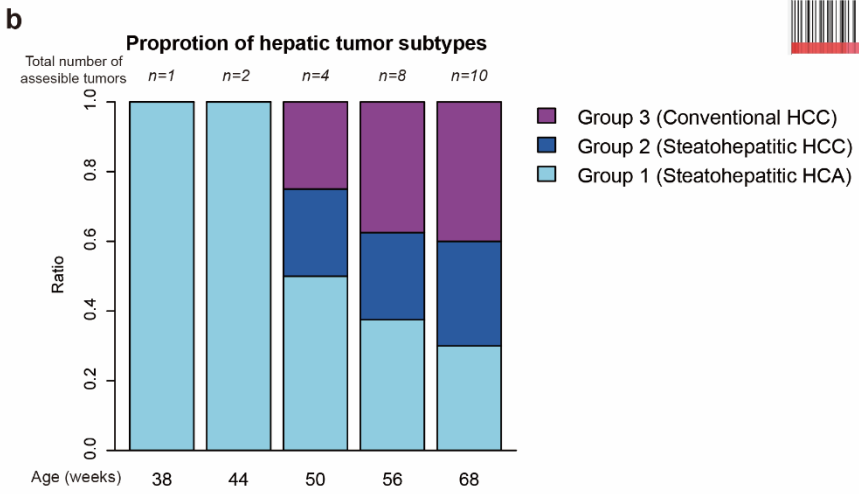
b
Proprotion of hepatic tumor subtypes
Total number of assesible tumors
n=1
n=2
n=4
n=8
n=10
Ratio
Age (weeks)
38
44
50
56
68
Group 3 (Conventional HCC)
Group 2 (Steatohepatitic HCC)
Group 1 (Steatohepatitic HCA)

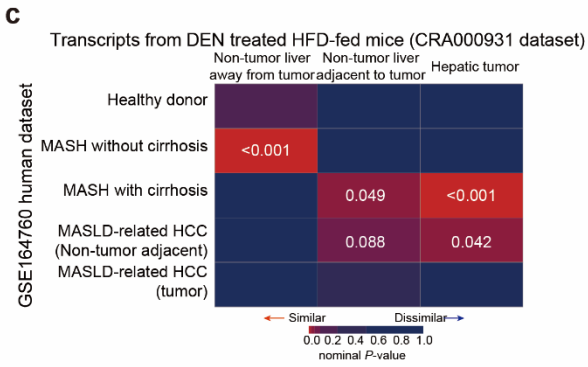
c
Transcripts from DEN treated HFD-fed mice (CRA000931 dataset)
Non-tumor liver away from tumor
Non-tumor liver adjacent to tumor
Hepatic tumor
GSE164760 human dataset
Healthy donor
MASH without cirrhosis
MASH with cirrhosis
MASLD-related HCC (Non-tumor adjacent)
MASLD-related HCC (tumor)
<0.001
0.049
<0.001
0.088
0.042
Similar
Dissimilar
nominal P-value

Supplementary Fig. 8. Molecular classification of hepatic tumors in STZ+HFD mice. (a) Gene set enrichment analysis in the 3 groups of hepatic tumors in STZ+HFD mouse using three different molecular classifications of human HCC. **(b)** Ratio of each hepatic tumor groups in different ages of STZ+HFD mice. **(c)** Submap clustering analyses comparing diethylnitrosamine-treated HFD-fed mice (CRA0000931) and human patients with MASLD-related HCC (GSE164760).

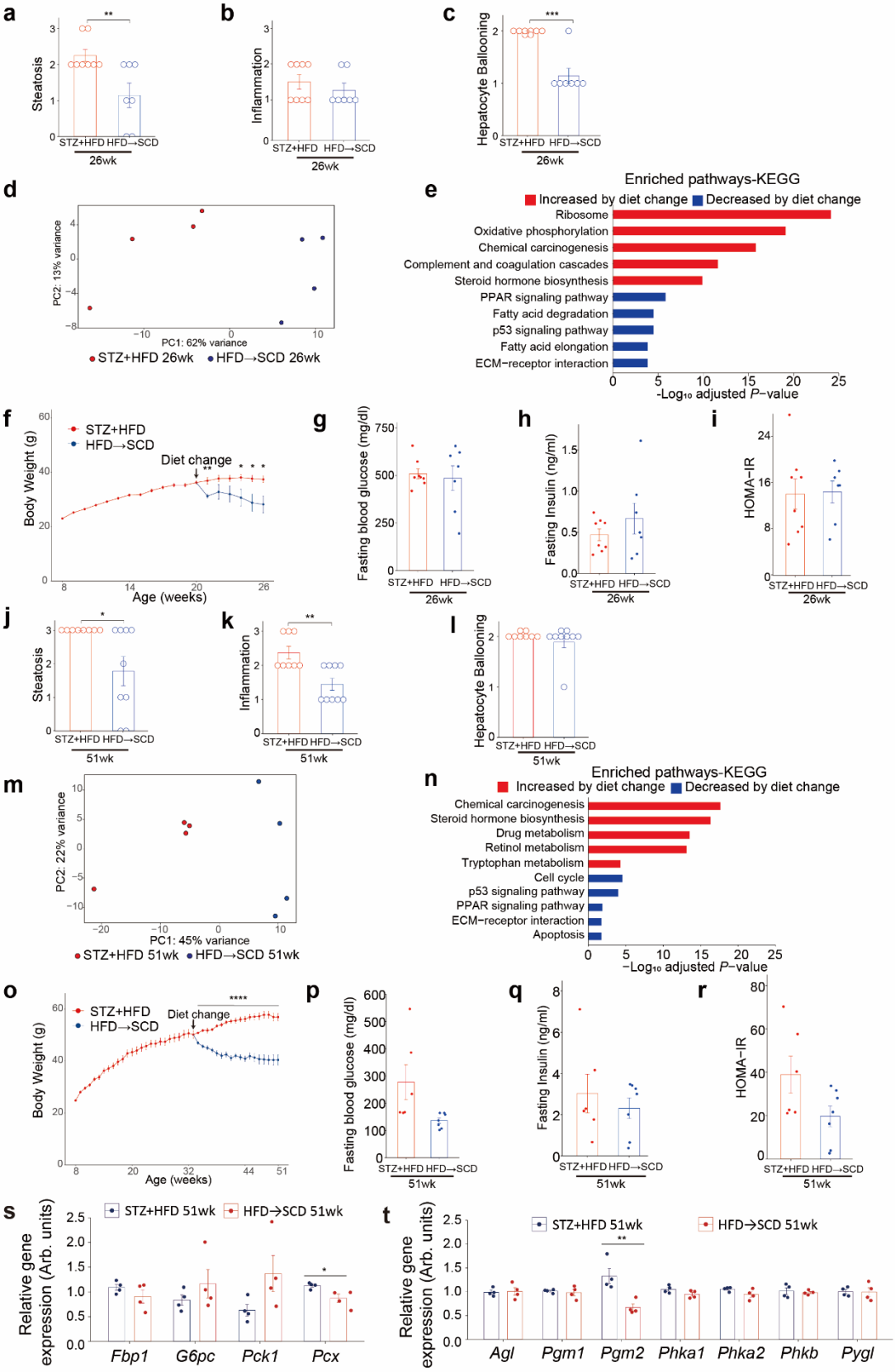
a
Steatosis
STZ+HFD
HFD→SCD
26wk
b
Inflammation
c
Hepatocyte Ballooning
d
PC2: 13% variance
PC1: 62% variance
STZ+HFD 26wk
HFD→SCD 26wk
e
Enriched pathways-KEGG
Increased by diet change
Decreased by diet change
Ribosome
Oxidative phosphorylation
Chemical carcinogenesis
Complement and coagulation cascades
Steroid hormone biosynthesis
PPAR signaling pathway
Fatty acid degradation
p53 signaling pathway
Fatty acid elongation
ECM−receptor interaction
-Log10 adjusted P−value
f
Body Weight (g)
Diet change
Age (weeks)
g
Fasting blood glucose (mg/dl)
h
Fasting Insulin (ng/ml)
i
HOMA−IR
j
51wk
k
l
m
PC2: 22% variance
PC1: 45% variance
n
Chemical carcinogenesis
Steroid hormone biosynthesis
Drug metabolism
Retinol metabolism
Tryptophan metabolism
Cell cycle
p53 signaling pathway
PPAR signaling pathway
ECM−receptor interaction
Apoptosis
o
p
q
r
s
Relative gene expression (Arb. units)
Fbp1
G6pc
Pck1
Pcx
t
Agl
Pgm1
Pgm2
Phka1
Phka2
Phkb
Pygl

Supplementary Fig. 9. Hepatic transcriptomic and metabolic phenotypes of STZ+HFD mice after dietary changes. (a-i) Seven-week-old B6J mice were treated with STZ, and fed HFD from 8 to 20 weeks, followed by HFD or SCD (HFD→SCD) until 26 weeks. **(a-c)** Detailed NAS grading with the NASH CRN scoring system; *n* = 8 for STZ+HFD, 7 for HFD→SCD. **(d)** Principal component analysis of RNA-seq data. **(e)** Functional enrichment analysis using KEGG pathways for differentially expressed genes (DEGs) following dietary changes. **(f-i)** Metabolic parameter changes including **(f)** body weight, **(g)** fasting blood glucose, **(h)** plasma insulin, **(i)** and HOMA-IR after 6 hours of fasting; *n* = 8 for STZ+HFD, 7 for HFD→SCD. **(j-r)** Seven-week-old B6J mice were treated with STZ and fed HFD from 8 to 33 weeks, followed by HFD or SCD (HFD→SCD) until 51 weeks. **(j-l)** Detailed NAS grading with the NASH CRN scoring system; *n* = 8 for STZ+HFD, 9 for HFD→SCD. **(m)** Principal component analysis of RNA-seq data. **(n)** Functional enrichment analysis using KEGG pathways for differentially expressed genes (DEGs) following dietary changes. **(o-r)** Metabolic parameter changes including **(o)** body weight, **(p)** fasting blood glucose, **(q)** plasma insulin, and **(r)** HOMA-IR after 6 hours of fasting; (**o**) *n* = 8 for STZ+HFD, 9 for HFD→SCD ; (**p-r**) *n* = 6 for STZ+HFD, 7 for HFD→SCD. (**s, t**) Relative expression (normalized reads from RNA-seq data) of genes related to (**s**) gluconeogenesis or (**t**) glycogenolysis in the livers following dietary changes; *n* = 4 per group (Arb. units; arbitrary units). Data are expressed as means ± SEM. $^{*}P<0.05$, $^{**}P<0.01$, $^{***}P<0.001$, $^{****}P<0.0001$, compared with age-matched group, Student's t-test or Welch's t-test **(a-c, f-l, o-t)**. Source data are provided as a Source Data file.

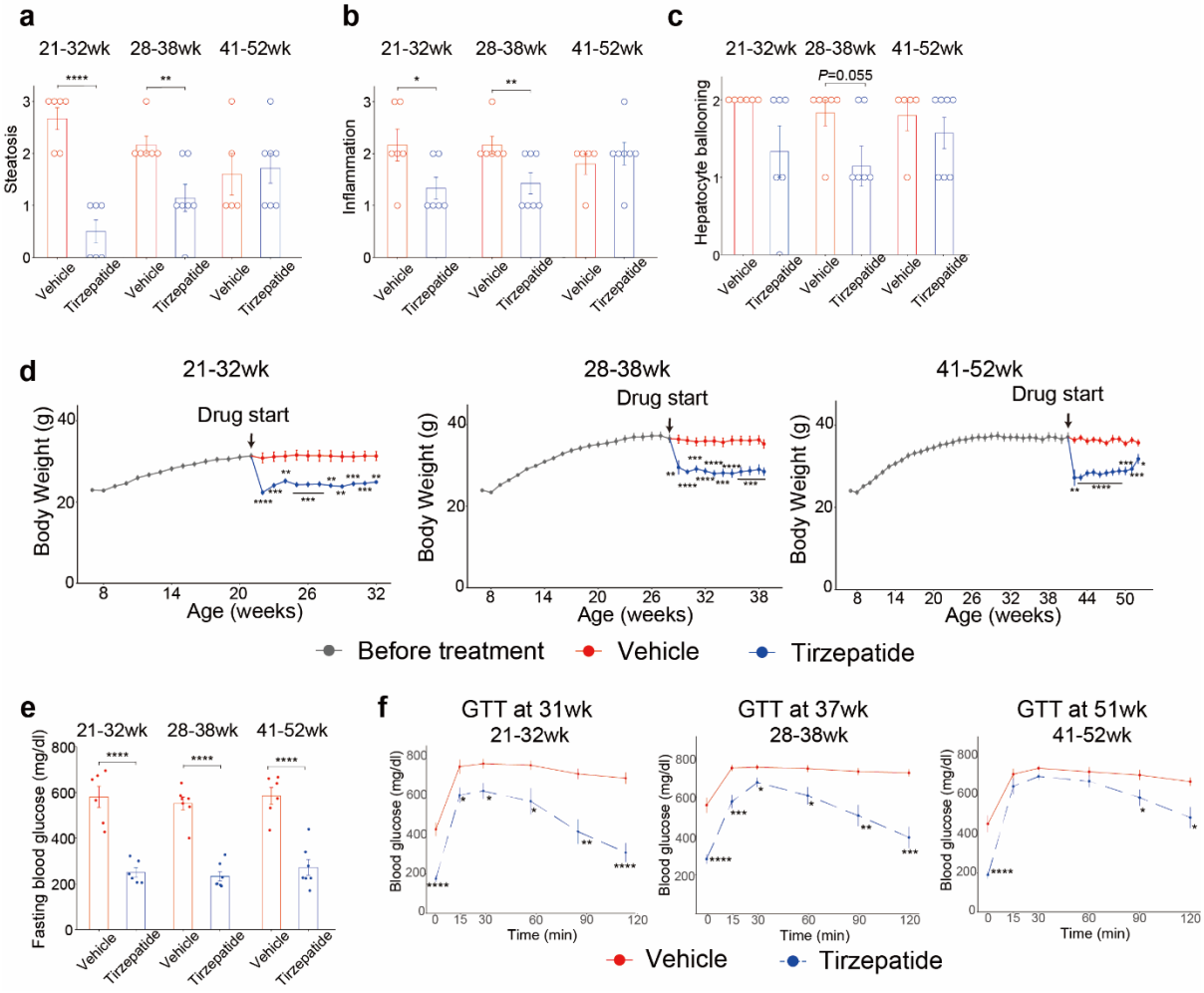
a
21-32wk
28-38wk
41-52wk
Steatosis
Vehicle
Tirzepatide
b
Inflammation
c
Hepatocyte ballooning
P=0.055
d
Drug start
Body Weight (g)
Age (weeks)
Before treatment
Vehicle
Tirzepatide
e
Fasting blood glucose (mg/dl)
f
GTT at 31wk
21-32wk
GTT at 37wk
28-38wk
GTT at 51wk
41-52wk
Blood glucose (mg/dl)
Time (min)

Supplementary Fig. 10. Metabolic phenotype of STZ+HFD mice after tirzepatide administration. (a-f) Seven-week-old B6J mice were treated with STZ, fed HFD from 8 weeks onwards and administered vehicle or tirzepatide for 10-11 weeks from 21, 28 or 41 weeks of age. **(a-c)** Detailed NAS grading using the NASH CRN scoring system; Vehicle, n = 6, 6, and 5, from 21-32 to 41-52 weeks, respectively; Tirzepatide, n = 6, 7, and 7, from 21-32 to 41-52 weeks, respectively. **(d)** Body weight trends; Vehicle, n = 6, 7, and 6, from 21-32 to 41-52 weeks, respectively; Tirzepatide, n = 6, 7, and 7, from 21-32 to 41-52 weeks, respectively. **(e)** Fasting blood glucose level; Vehicle, n = 6, 7, and 5, from 21-32 to 41-52 weeks, respectively; Tirzepatide, n = 6, 7, and 7, from 21-32 to 41-52 weeks, respectively. **(f)** Intraperitoneal glucose tolerance test (IPGTT) after 14 h of fasting at 31, 37 or 51 weeks of age; Vehicle, n = 6, 7, and 6, from 31 to 51 weeks, respectively; Tirzepatide, n = 6, 7, and 7, from 31 to 51 weeks, respectively. Data are expressed as means ± SEM. $^{*}P<0.05$, $^{**}P<0.01$, $^{***}P<0.001$, $^{****}P<0.0001$, compared with age-matched group, Student's t-test or Welch's t-test **(a-f)**. Source data are provided as a Source Data file.

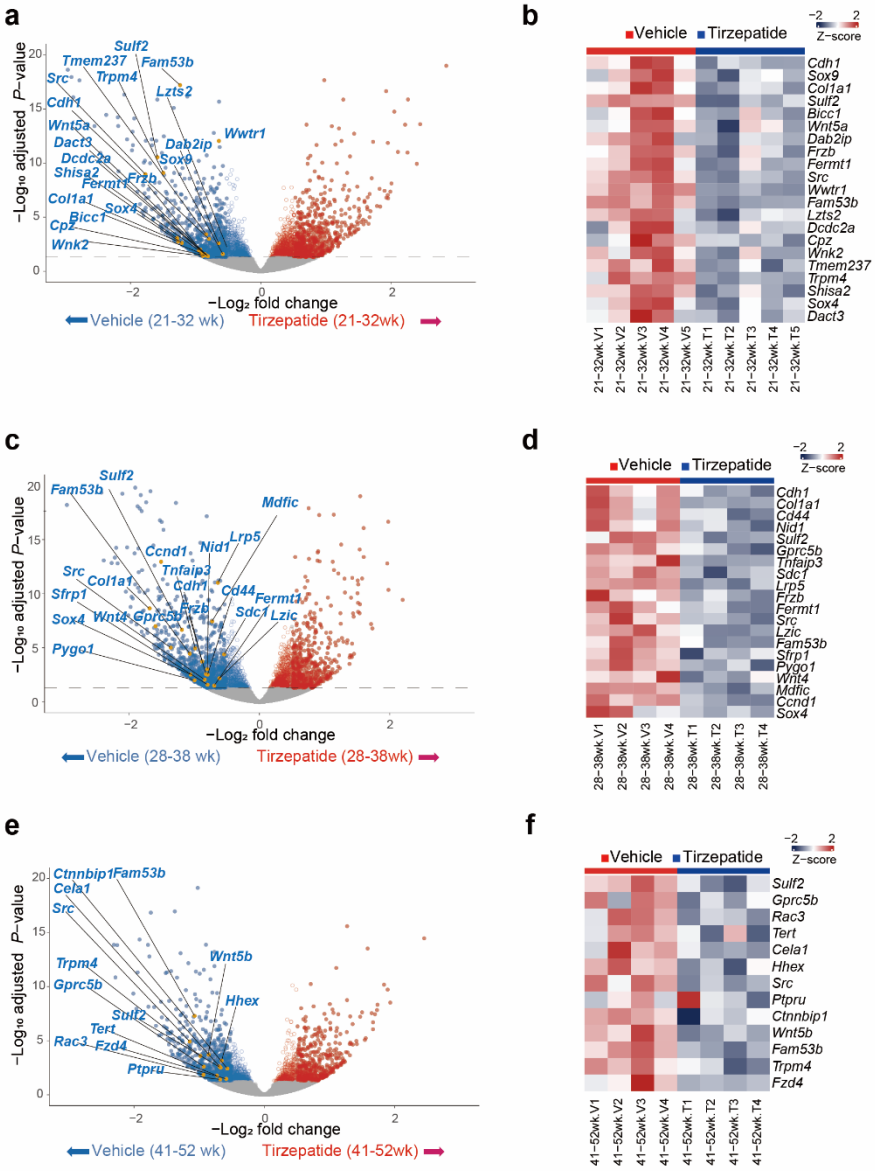
a
Sulf2
Tmem237
Fam53b
Src
Trpm4
Lzts2
Cdh1
Wnt5a
Wwtr1
Dact3
Dab2ip
Dcdc2a
Sox9
Shisa2
Frzb
Fermt1
Col1a1
Sox4
Bicc1
Cpz
Wnk2
−Log₁₀ adjusted P−value
−Log₂ fold change
Vehicle (21-32 wk)
Tirzepatide (21-32wk)
b
Vehicle
Tirzepatide
Z−score
Cdh1
Sox9
Col1a1
Sulf2
Bicc1
Wnt5a
Dab2ip
Frzb
Fermt1
Src
Wwtr1
Fam53b
Lzts2
Dcdc2a
Cpz
Wnk2
Tmem237
Trpm4
Shisa2
Sox4
Dact3
21−32wk.V1
21−32wk.V2
21−32wk.V3
21−32wk.V4
21−32wk.V5
21−32wk.T1
21−32wk.T2
21−32wk.T3
21−32wk.T4
21−32wk.T5
c
Sulf2
Fam53b
Mdfic
Lrp5
Ccnd1
Nid1
Src
Col1a1
Tnfaip3
Cdh1
Cd44
Sfrp1
Fermt1
Frzb
Sdc1
Lzic
Sox4
Wnt4
Gprc5b
Pygo1
−Log₁₀ adjusted P−value
−Log₂ fold change
Vehicle (28-38 wk)
Tirzepatide (28-38wk)
d
Vehicle
Tirzepatide
Z−score
Cdh1
Col1a1
Cd44
Nid1
Sulf2
Gprc5b
Tnfaip3
Sdc1
Lrp5
Frzb
Fermt1
Src
Lzic
Fam53b
Sfrp1
Pygo1
Wnt4
Mdfic
Ccnd1
Sox4
28−38wk.V1
28−38wk.V2
28−38wk.V3
28−38wk.V4
28−38wk.T1
28−38wk.T2
28−38wk.T3
28−38wk.T4
e
Ctnnbip1
Fam53b
Cela1
Src
Wnt5b
Trpm4
Gprc5b
Hhex
Sulf2
Tert
Rac3
Fzd4
Ptpru
−Log₁₀ adjusted P−value
−Log₂ fold change
Vehicle (41-52 wk)
Tirzepatide (41-52wk)
f
Vehicle
Tirzepatide
Z−score
Sulf2
Gprc5b
Rac3
Tert
Cela1
Hhex
Src
Ptpru
Ctnnbip1
Wnt5b
Fam53b
Trpm4
Fzd4
41−52wk.V1
41−52wk.V2
41−52wk.V3
41−52wk.V4
41−52wk.T1
41−52wk.T2
41−52wk.T3
41−52wk.T4

Supplementary Fig. 11. Transcriptomic analysis of Wnt signaling pathway in liver of vehicle- and tirzepatide-administered mice. (a-f) (**a, c, e**) Volcano plot and (**b, d, f**) heatmap showing significantly decreased genes related to Wnt signaling pathways included in GO: 0016055 series, after tirzepatide administration (**a, b**: treated during 21-32 weeks; **c, d**: 28-38 weeks; **e, f**: 41-52 weeks).

Supplementary Table 1. Clinical characteristics of healthy donors and MASLD patients

	Healthy donor (n=4)	MASLD patients (n=28)
Age (yr) mean ± S.D.	26.3 ± 6.9	43 ± 15.6
Sex		
Male (n)	4 (100 %)	19 (67.9 %)
Female (n)	0 (0 %)	9 (32.1 %)
Diabetes (n)	0 (0 %)	11 (39.3 %)
Distribution of NAS		
0	4	0
1		0
2		2
3		4
4		4
5		11
6		5
7		2
Distribution of fibrosis stage		
0	4	0
1a		6
1b		5
2		5
3		6
4		6
BMI (kg/m^2) mean ± S.D.	24.5 ± 2.4	29.8 ± 5.3
Body fat mass (%)	26.6 ± 6.3	34.1 ± 7.4
AST (IU/L)	16 ± 4.9	76 ± 70.8
ALT (IU/L)	15. ± 4.7	91.2 ± 95.3
γ-GTP (IU/L)	20.8 ± 4.9	139 ± 182.9
Total cholesterol (mg/dL)	174.3 ± 46.8	188.2 ± 40.8
Triglyceride (mg/dL)	94 ± 31	195.4 ± 98
HDL-cholesterol (mg/dL)	45.5 ± 10.8	43.3 ± 7.7
LDL-cholesterol (mg/dL)	118.5 ± 45.6	98.7 ± 44.5

Supplementary Table 2. Histological background of liver at the time of hepatic tumor identification in STZ+HFD mice

Histologic features	Score	Number of mice with hepatic tumor development (%)
Steatosis	0	0 (0)
	1	2 (8.7)
	2	9 (39.1)
	3	12 (52.2)
Inflammation	0	1 (4.4)
	1	11 (47.8)
	2	11 (47.8)
	3	0 (0)
Hepatocyte ballooning	0	0 (0)
	1	3 (13)
	2	20 (87)
Total NAS	2	1 (4.4)
	4	2 (8.7)
	5	4 (17.4)
	6	10 (43.5)
	7	6 (26.1)
Fibrosis stage	0	0 (0)
	1	2 (8.7)
	2	9 (39.1)
	3	10 (43.5)
	4	2 (8.7)

Supplementary Table 3. Histopathological characteristics of developing hepatic tumors in STZ+HFD mice

ID/Group	Age(weeks)	Maximum tumor diameter (cm)	Histologic type	Image	NAS (Background liver)	Fibrosis stage (Background liver)
Tumor3/ Group1	44	0.2	Steatohepatitic HCA	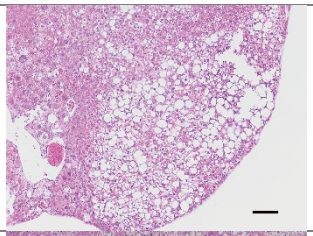	6	2
Tumor4/ Group1	44	0.3	Steatohepatitic HCA	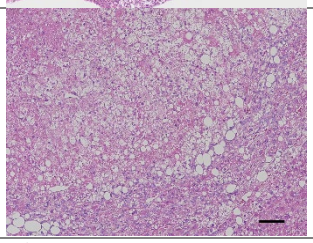	6	2
Tumor5/ Group1	44	0.2	N/A	N/A	5	4
Tumor6/ Group1	44	0.3	N/A	N/A	7	3
Tumor7/ Group2	50	0.5	Steatohepatitic HCC	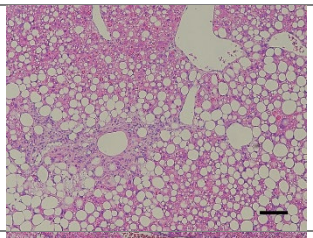	6	2
Tumor9/ Group1	50	0.3	Steatohepatitic HCA	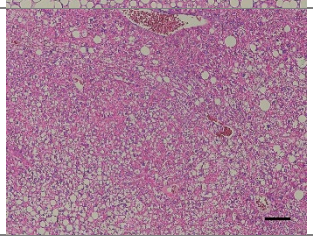	6	2
Tumor10/ Group1	50	0.3	N/A	N/A	6	2
Tumor11/ Group3	50	2.1	Conventional HCC	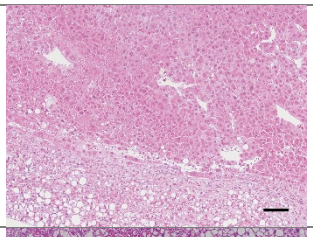	4	3
Tumor13/ Group1	56	0.4	Steatohepatitic HCA	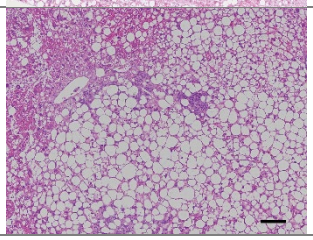	6	3

Tumor14/ Group3	56	0.7	Conventional HCC	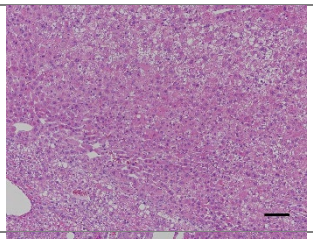	7	3
Tumor18/ Group3	56	0.9	Conventional HCC	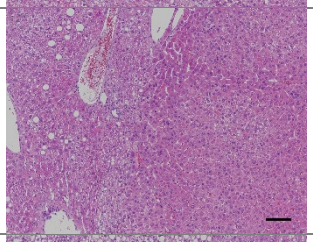	5	1b
Tumor22/ Group2	56	0.4	Steatohepatitic HCC	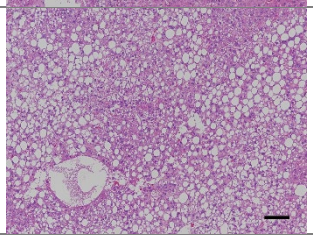	7	3
Tumor24/ Group1	56	0.2	N/A	N/A	7	2
Tumor25/ Group2	56	0.3	Steatohepatitic HCC	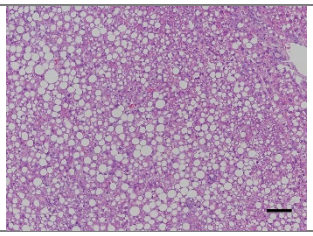	7	2

*N/A signifies not accessible due to small tumor size. HCA, Hepatocellular adenoma; HCC; Hepatocellular carcinoma. Scale bar, 100 μm.

Supplementary Table 4. Entire significant results (adjusted p-value <0.05) of functional enrichment analysis using KEGG pathways for downregulated genes of 26-week-old mice following 6 weeks of diet change to chow compared to mice continued high fat diet.

KEGG pathway	P-value	Adjusted p-value	Odds Ratio	Combined score
PPAR signaling pathway	5.71.E-09	1.57.E-06	5.63	106.94
p53 signaling pathway	2.61.E-07	3.43.E-05	5.39	81.68
Fatty acid degradation	3.74.E-07	3.43.E-05	6.64	98.33
Fatty acid elongation	2.14.E-06	1.47.E-04	8.97	117.08
ECM-receptor interaction	2.73.E-06	1.50.E-04	4.41	56.46
Cell cycle	1.53.E-05	6.99.E-04	3.32	36.87
Proteoglycans in cancer	2.53.E-05	9.93.E-04	2.63	27.87
Focal adhesion	4.83.E-05	1.66.E-03	2.58	25.62
Biosynthesis of unsaturated fatty acids	2.92.E-04	8.91.E-03	5.67	46.14
AGE-RAGE signaling pathway in diabetic complications	4.74.E-04	1.19.E-02	2.98	22.77
Osteoclast differentiation	7.73.E-04	1.77.E-02	2.61	18.73
PI3K-Akt signaling pathway	9.02.E-04	1.91.E-02	1.86	13.07
Phagosome	1.13.E-03	2.22.E-02	2.26	15.32
C-type lectin receptor signaling pathway	1.41.E-03	2.59.E-02	2.64	17.3
Platelet activation	1.62.E-03	2.78.E-02	2.5	16.09
TNF signaling pathway	3.25.E-03	4.59.E-02	2.48	14.23
Primary immunodeficiency	3.34.E-03	4.59.E-02	4.1	23.38

Supplementary Table 5. Entire significant results (adjusted p-value <0.05) of functional enrichment analysis using KEGG pathways for upregulated genes of 26-week-old mice following 6 weeks of diet change to chow compared to mice continued high fat diet.

KEGG pathway	P-value	Adjusted p-value	Odds Ratio	Combined score
Ribosome	2.78.E-27	8.03.E-25	7.87	480.93
Oxidative phosphorylation	4.96.E-22	7.16.E-20	7.87	386.18
Chemical carcinogenesis	2.16.E-18	1.56.E-16	8.87	360.74
Complement and coagulation cascades	7.17.E-14	2.59.E-12	7.31	221.35
Thermogenesis	3.02.E-13	9.70.E-12	3.94	113.48
Steroid hormone biosynthesis	4.82.E-12	1.39.E-10	6.47	168.55
Steroid biosynthesis	5.54.E-12	1.46.E-10	31.92	827.36
Retinol metabolism	5.38.E-11	1.30.E-09	5.94	140.35
Drug metabolism	2.33.E-09	5.19.E-08	4.6	91.49
Metabolism of xenobiotics by cytochrome P450	2.85.E-09	5.89.E-08	6.43	126.46
Linoleic acid metabolism	3.15.E-07	6.07.E-06	6.31	94.53
Cysteine and methionine metabolism	1.97.E-06	3.55.E-05	5.72	75.23
Glycine, serine and threonine metabolism	4.79.E-06	8.15.E-05	6.3	77.19
Terpenoid backbone biosynthesis	6.43.E-06	1.03.E-04	9.44	112.83
Tryptophan metabolism	6.83.E-06	1.04.E-04	5.46	64.98
Glutathione metabolism	9.55.E-06	1.38.E-04	4.51	52.1
Arginine biosynthesis	1.12.E-05	1.53.E-04	10.67	121.63
Arachidonic acid metabolism	1.17.E-05	1.53.E-04	3.74	42.45
Glyoxylate and dicarboxylate metabolism	1.46.E-05	1.83.E-04	6.99	77.88

Peroxisome	2.01.E-05	2.38.E-04	3.74	40.43
Folate biosynthesis	2.06.E-05	2.38.E-04	7.77	83.84
Cholesterol metabolism	4.62.E-05	5.14.E-04	4.77	47.58
Selenocompound metabolism	4.83.E-05	5.17.E-04	10.26	101.99
Retrograde endocannabinoid signaling	8.56.E-05	8.83.E-04	2.67	25.03
Fatty acid biosynthesis	1.32.E-04	1.32.E-03	10.99	98.14
Tyrosine metabolism	1.64.E-04	1.58.E-03	4.89	42.65
Glycerophospholipid metabolism	1.27.E-03	1.18.E-02	2.69	17.93
Cardiac muscle contraction	1.30.E-03	1.18.E-02	2.94	19.52
Serotonergic synapse	1.94.E-03	1.67.E-02	2.32	14.5
Bile secretion	1.97.E-03	1.67.E-02	2.94	18.29
Primary bile acid biosynthesis	2.59.E-03	2.14.E-02	6.65	39.62
Histidine metabolism	3.41.E-03	2.73.E-02	4.88	27.74
Fatty acid degradation	4.12.E-03	3.22.E-02	3.22	17.67

Supplementary Table 6. Entire significant results (adjusted p-value <0.05) of functional enrichment analysis using KEGG pathways for downregulated genes of 51-week-old mice following 18 weeks of diet change to chow compared to mice continued high fat diet.

KEGG pathway	P-value	Adjusted p-value	Odds Ratio	Combined score
Cell cycle	1.12.E-07	2.95.E-05	4.69	74.98
p53 signaling pathway	8.15.E-07	1.07.E-04	5.9	82.66
PPAR signaling pathway	1.58.E-04	1.38.E-02	3.93	34.43
Oocyte meiosis	2.54.E-04	1.44.E-02	3.29	27.21
Progesterone-mediated oocyte maturation	2.73.E-04	1.44.E-02	3.68	30.19
ECM-receptor interaction	5.12.E-04	1.90.E-02	3.65	27.66
Apoptosis	6.14.E-04	1.90.E-02	2.85	21.09
Amino sugar and nucleotide sugar metabolism	7.28.E-04	1.90.E-02	4.65	33.62
Hippo signaling pathway	7.57.E-04	1.90.E-02	2.68	19.26
AGE-RAGE signaling pathway in diabetic complications	7.93.E-04	1.90.E-02	3.22	23.01
Focal adhesion	1.28.E-03	2.59.E-02	2.38	15.88

Supplementary Table 7. Entire significant results (adjusted p-value <0.05) of functional enrichment analysis using KEGG pathways for upregulated genes of 51-week-old mice following 18 weeks of diet change to chow compared to mice continued high fat diet.

KEGG pathway	P-value	Adjusted p-value	Odds Ratio	Combined score
Chemical carcinogenesis	1.09E-20	2.76E-18	13.67	628.56
Steroid hormone biosynthesis	3.86E-19	4.90E-17	13.31	564.17
Drug metabolism	4.10E-16	3.47E-14	9.47	335.54
Retinol metabolism	1.29E-15	8.18E-14	10.89	373.38
Metabolism of xenobiotics by cytochrome P450	2.11E-13	1.07E-11	12.21	356.25
Ascorbate and aldarate metabolism	1.18E-07	4.99E-06	14.89	237.52
Linoleic acid metabolism	5.22E-07	1.89E-05	8.41	121.72
Tryptophan metabolism	2.93E-06	9.31E-05	7.84	99.88
Porphyrin and chlorophyll metabolism	5.83E-06	1.65E-04	8.37	100.85
Arachidonic acid metabolism	6.64E-06	1.69E-04	5.11	60.92
Pentose and glucuronate interconversions	1.12E-05	2.58E-04	9.14	104.24
Tyrosine metabolism	3.98E-05	8.43E-04	7.43	75.24
Phenylalanine metabolism	7.75E-05	1.51E-03	10.46	99.02
Peroxisome	9.43E-05	1.71E-03	4.49	41.6
Primary bile acid biosynthesis	1.23E-04	2.08E-03	13.46	121.19
Serotonergic synapse	4.19E-04	6.65E-03	3.26	25.32
Inflammatory mediator regulation of TRP channels	9.97E-04	1.49E-02	3.11	21.46
Glutathione metabolism	1.15E-03	1.58E-02	4.24	28.7
Fatty acid degradation	1.18E-03	1.58E-02	4.83	32.54

Glycine, serine and threonine metabolism	1.83E-03	2.27E-02	5.23	32.93
Nitrogen metabolism	1.96E-03	2.27E-02	9.09	56.69
Selenocompound metabolism	1.96E-03	2.27E-02	9.09	56.69
Bile secretion	2.47E-03	2.72E-02	3.71	22.26